

Wetting dynamics: two simple models

This article has been downloaded from IOPscience. Please scroll down to see the full text article.

1991 J. Phys. A: Math. Gen. 24 L351

(<http://iopscience.iop.org/0305-4470/24/7/007>)

View [the table of contents for this issue](#), or go to the [journal homepage](#) for more

Download details:

IP Address: 129.252.86.83

The article was downloaded on 01/06/2010 at 14:11

Please note that [terms and conditions apply](#).

LETTER TO THE EDITOR

Wetting dynamics: two simple models

Joanna Cook and Dietrich E Wolf

Institut für Festkörperforschung, Forschungszentrum Jülich, POB 1913, D-W 5170 Jülich, Federal Republic of Germany

Received 2 January 1991

Abstract. Two models of the wetting dynamics of a non-volatile liquid are introduced. Both models exhibit a transition between partial and complete wetting regimes. The first model, which can also be viewed as an inhomogeneous surface growth model, is studied in a two-dimensional capillary geometry. For complete wetting the profile of the fluid surface, apart from a precursor film, then assumes a stationary shape, which scales with the system size. A precursor film forms even at the transition, which one can locate analytically, although here it moves only as t^χ , where $\chi \approx 1/2$. This first model permits only fluctuations parallel to the wall over which the fluid spreads. Monte Carlo simulations of the second model show that the inclusion of fluctuations perpendicular to the wall can lead to qualitatively new phenomena.

Wetting phenomena involve three coexisting phases, e.g., a solid wall A, a liquid B and a gas C. Usually, one can ignore the exchange of particles between the solid wall and the fluid phases. One may then distinguish two different ensembles for the wetting dynamics: (i) partial chemical equilibrium between the liquid B and the gas C [1], and (ii) hindered or blocked chemical equilibrium between B and C which applies, e.g., to the spreading of a non-volatile liquid [2]. In this letter we consider case (ii) for the two geometries depicted in figure 1.

In the first case (figure 1(a)), a geometry employed in recent models to study the wetting dynamics [3, 4], one has two parallel plates made of phase A. The upper plate ends at $y=0$, while the lower one extends to infinity. The gap between the two plates is connected to a reservoir of liquid B. Initially the liquid-gas interface is planar and lies at $y=0$, perpendicular to the plates. If the surface tension of the wall-gas interface is larger than that of the wall-liquid interface, $\mu = \sigma_{AC} - \sigma_{AB} > 0$, the liquid will flow out of the gap between the plates, the upper end of the liquid-gas interface remaining

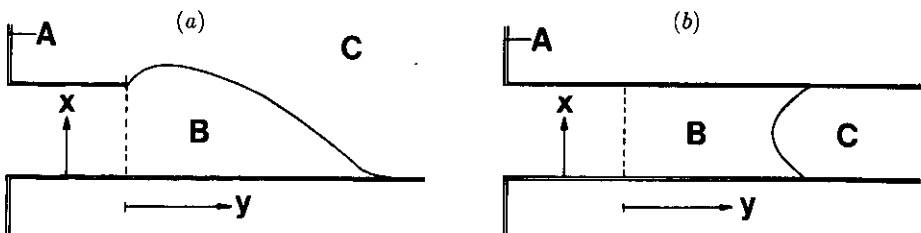


Figure 1. The two geometries employed in our simulations. (a) Shows the geometry used both for our second model and in [3, 4, 6]. (b) Illustrates the capillary geometry used for our first model.

pinned at the edge of the upper plate. Two regimes can be distinguished: for $0 < \mu < \sigma = \sigma_{BC}$ the fluid surface adopts a static profile making a non-zero contact angle with the lower plate, according to Young's law [2] (partial wetting). For $\mu > \sigma$ the system exhibits complete wetting: the contact angle vanishes and the fluid spreads over the surface, the main body of the fluid preceded by a precursor film [3, 5].

In the model introduced by Abraham *et al* it was found [3, 4] that the profile behind the precursor film does not approach a stationary limit. One may ask whether this is generally true or a consequence of the geometry with one end of the fluid surface pinned. Therefore, we have studied an alternative model of wetting dynamics in the capillary geometry of figure 1(b). (This arrangement has already been considered for partial wetting in [6].) In this geometry both plates extend to infinity. The gap between the plates is filled with gas, and initially the liquid-gas interface is oriented perpendicular to the plates. Our model also exhibits a transition between partial and complete wetting. However, in the case of complete wetting, if one excludes the precursor film, the fluid surface approaches a stationary limit. We see a precursor even at the transition, but its properties are different than for complete wetting.

The models studied in [3, 4, 6] and the first model we shall discuss here all excluded fluctuations perpendicular to the walls. In the second part of this letter we shall show that these fluctuations can lead to the new phenomenon of a drop forming at the mouth of the reservoir in figure 1(a).

Consider the Langevin equation

$$\partial h / \partial t = \sigma \nabla^2 h + \kappa + \mu (\delta(x) + \delta(x-L)) + \eta \quad (1)$$

where $\eta(x, t)$ is Gaussian white noise. This equation (with $\kappa = 0$) can be interpreted as the linear approximation of the dynamics of a fluid surface at $y = h(x, t)$ in a capillary with walls at $x = 0$ and $x = L$. This approximation is only good for small gradients of h .

Alternatively, one can view (1) as a continuum approximation of the Edwards-Wilkinson (EW) model [7] of a surface growing via inhomogeneous deposition of particles [8]. On the square lattice this model is defined in the following way [9]. One has a one-dimensional substrate with sites $x = 1, \dots, L$ with periodic boundary conditions, $h(0, t) = h(L, t)$, for the integer surface height. Particles are added one by one on top of randomly chosen columns $x = \text{constant}$, where they only stick provided that none of the neighbouring columns is lower. Otherwise, they move to the lowest of the two neighbouring columns (or to one of these chosen at random, if these heights are equal) and stick there. Sticking means that the corresponding height increases by 1. The deposition is made inhomogeneous by selecting site $x = L$ with a probability $(p+1)/(p+L)$ whilst all other sites are only chosen with probability $1/(p+L)$. If one adds $p+L$ particles per unit time, the average deposition rate in (1) is $\kappa = 1$, whereas the extra deposition at the boundaries amounts to $\mu = p/2$. As κ can be transformed away in a comoving frame, this growth model can be used to investigate the meniscus of a fluid in a capillary. Again, the linear continuum approximation (1) is only good for small surface gradients. This is why the solutions of (1) always have a non-zero contact angle [6, 8].

We have performed simulations of the EW model in order to look for a 'wetting' transition. The simulations were run on an IBM 3090 for system sizes between $L = 10$ and $L = 100$ and the results were averaged over many independent runs (typically of the order of a few hundred). A transition was found at

$$p_c = 2L/(L-3). \quad (2)$$

For $0 < p < p_c$ the system adopted a steady state with non-zero contact angles. For values of p considerably less than p_c the meniscus was parabolic as predicted by (1). However, for larger values of p the profile only remained parabolic towards the centre of the system where the slope is small. The steady-state profile advanced at a velocity p/L (in the following, velocities are always given in the frame where $\kappa = 0$). The reason is that there is an extra deposition of p particles per unit time which makes all L sites move faster by the same amount. In the language of a fluid, this corresponds to the velocity of the capillary rise and, as it should be, it is inversely proportional to the width of the capillary or radius of curvature of the meniscus.

For $p > p_c$ a precursor, three sites wide, was observed at the edges of the capillary. The height of the precursor grows with velocity v_p , and the rest of the system approaches a stationary profile which advances at a smaller velocity, v . The width of the precursor is a simple consequence of the deposition rule implemented. The extra deposition only occurs at site L , but when $h(L) > h(L-1)$ or $h(L) > h(1)$ these extra particles are added at site $L-1$ or 1 rather than site L . Therefore, if a precursor forms it must be three sites wide. The precursor decouples from the rest of the system: as its height, relative to the height at the centre of the system increases, the probability of a fluctuation bringing $h(2)$ or $h(L-2)$ up to the precursor height becomes negligible. The precursor can then only grow when site L is chosen as the deposition site. Particles added at the two other sites of the precursor do not contribute to its velocity, but rather to the velocity of the meniscus left behind. Hence the velocity of the precursor, v_p , and that of the rest of the profile, v , are

$$v_p = (p-2)/3 \quad v = 2/(L-3). \quad (3)$$

At the transition one must have $v_p = v = p_c/L$ in agreement with our numerical finding (2).

As was also the case below p_c , the stationary part of the profile has a scaling form for large L and t , $h(x, t) = Lf(x/L) + vt$. This is illustrated in figure 2, where the data for $L=80$ and $L=100$ collapse. For $L=40$ there are still finite-size corrections visible. The stationary profile will be independent of p , as increasing p beyond p_c simply feeds

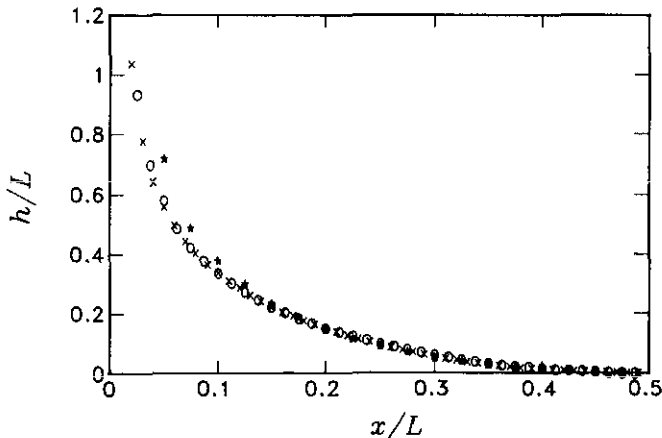


Figure 2. The scaled stationary part of the profile obtained in the complete wetting regime. The data are from simulations with $p=3$ and system sizes $L=40$ (stars), $L=80$ (circles) and $L=100$ (crosses).

the extra particles into the precursor. We have checked that at p_c the stationary part of the profile agrees with the curve on figure 2.

A precursor still develops when $p = p_c$, but its height, relative to the height at the centre of the system, now grows as t^χ rather than with a constant velocity. It was necessary to wait very long times until the transients had died out sufficiently to be able to evaluate the asymptotic exponent. Figure 3 shows a double logarithmic plot, for system sizes $L=10$ and $L=40$. Fitting these data to a straight line we obtain $\chi = 0.48 \pm 0.02$. This suggests that $\chi = 1/2$, which is expected, if this effect is merely due to fluctuations in the number of particles deposited on the precursor relative to the average.

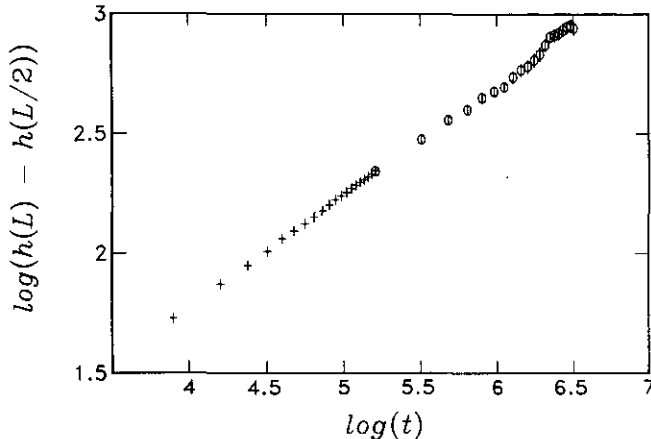


Figure 3. A double logarithmic plot of the time dependence of the precursor height, measured relative to the centre of the profile, at $p = p_c$. The system sizes are $L = 10$ (crosses) where the error bars are smaller than the symbol size, and $L = 40$ (circles).

We shall now briefly discuss the second model of a spreading fluid. In order to investigate the possible consequences of including fluctuations both parallel and perpendicular to the walls, we have investigated a two-dimensional model in which the liquid-gas interface is represented by a self-avoiding walk (SAW) [10, 11]. We have adopted the geometry of figure 1(a). We commence with the fluid surface lying on the line $y = 0$, perpendicular to the walls, which are separated by L lattice constants. One end of the SAW is fixed at $(x, y) = (L, 0)$, as the fluid surface is pinned at the edge of the upper plate. The other end is constrained to sit on the lower wall, at $(0, Y)$. Therefore Y corresponds to the distance up to which the fluid has spread. A Monte Carlo simulation was performed, weighting the different SAW (surface) configurations by Boltzmann factors with energy

$$H = \sigma N - \mu Y - (\sigma - \mu)M. \quad (4)$$

The length of the surface, or number of bonds N contained in the SAW, may vary between L and infinity. M is the number of holes in the precursor film, corresponding to the number of bonds of the SAW that lie directly on the lower wall. It can be ignored in the following, as it has no bearing on the phenomena we wish to discuss.

Simulations were performed for various values of $\tilde{\sigma} = \sigma/T$ and $\tilde{\mu} = \mu/T$, where T is the temperature. $\tilde{\sigma}$ was always large enough to prevent the SAW proliferating to fill

out the lattice, i.e. we are not close to the critical point of liquid-gas coexistence [11]. A transition was found when $\tilde{\sigma} = \tilde{\mu}$. If $\tilde{\sigma} > \tilde{\mu}$, one observes partial wetting. On average the SAW adopts a stationary state with a non-zero contact angle with the wall. If $\tilde{\mu} > \tilde{\sigma}$, complete wetting occurs and the displacement Y grows linearly with time. If $\tilde{\sigma}$ is rather large, say $\tilde{\sigma} \approx 5$, then the profile of the fluid essentially looks similar to that found in Abraham's model [3, 4], at least for times accessible to our computer simulation. However, there is no longer a precursor of constant thickness, due to the fluctuations present in the model. As the surface tension σ is decreased, all traces of a thin 'precursor'-like structure disappear, and a drop of fluid develops at the mouth of the reservoir. The spreading potential continues to drive the end of the SAW to larger displacements Y , and simultaneously the gain in entropy makes the fluid surface bulge out away from the wall. An example of this phenomenon is shown in figure 4 for $L = 2$, $\tilde{\sigma} = 1.5$, $\tilde{\mu} = 1.65$. To observe this within easily accessible times we have taken L and $\tilde{\sigma}$ to be very small. However, the same phenomenon should occur for larger L or $\tilde{\sigma}$, although one would have to go to much longer times to be able to detect it.

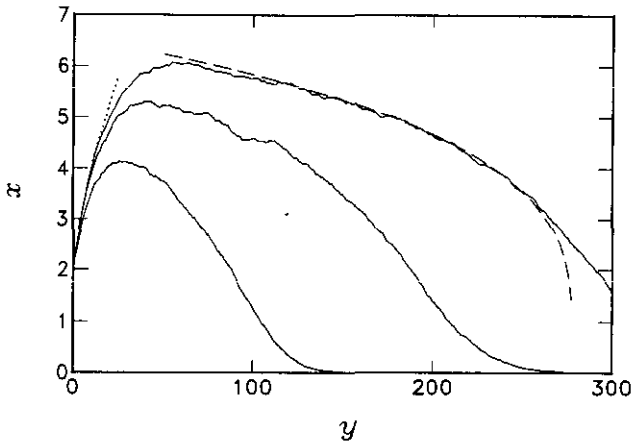


Figure 4. The full curves show the profile of the fluid surface at three equally spaced times for $L = 2$, $\tilde{\sigma} = 1.5$, $\tilde{\mu} = 1.65$. The profile for the longest time is averaged over 3900 runs and the profiles for the two earlier times are averaged over 1500 runs. Also shown are the fits $x = 1.08(y + 3.4)^{0.50}$ (dotted curve) and $x = 1.44(278 - y)^{0.27}$ (broken curve).

The shape of the drop is produced by the entropic repulsion of the fluid surface from the wall. One can therefore postulate that the shape should follow simple scaling forms. It is known [1] that within a time t thermal fluctuations develop on a planar surface up to a distance $\xi \sim t^{1/z}$ with $z = 2$. Their amplitude increases as ξ^ζ with $\zeta = 1/2$ in two dimensions. As the surface is pinned at $y = 0$, only fluctuations up to wavelength y contribute to the average surface displacement $x(y)$ at a distance y from this point. Hence one should get, for $1 \ll y \ll t^{1/2}$,

$$x(y) \sim y^\zeta. \tag{5}$$

At the opposite end of the drop, a distance $\tilde{y} = vt - y$ back from its foot, which propagates at velocity v , the surface fluctuations have had a time \tilde{y}/v to develop. Hence, one expects that for $t^{1/2} \ll y \ll vt$ the shape of the drop scales as

$$x(y) \sim (vt - y)^{\zeta/z}. \tag{6}$$

We have fitted our data to expressions (5) and (6), adjusting the exponent, the proportionality factor and a shift of the coordinate y . The best fits have been superimposed on the data in figure 4 and seem to be consistent with the simple scaling ideas, although, especially in the case of (5), much larger systems would be needed to provide conclusive evidence.

In three dimensions this phenomenon will be less pronounced, as the surface fluctuations increase only logarithmically with distance. Hence (5) and (6) will be replaced by logarithmic dependencies.

We wish to thank D Abraham, R Lipowsky, B Chopard, K Kaski, H Herrmann and P Devillard for stimulating discussions. This work was supported by the Deutsche Forschungsgemeinschaft within SFB 341. JC acknowledges the support of the Royal Society.

References

- [1] Lipowsky R 1985 *J. Phys. A: Math. Gen.* **18** L585; 1988 *Random Fluctuations and Growth* ed H E Stanley and N Ostrowsky (Dordrecht: Kluwer)
- [2] de Gennes P G 1985 *Rev. Mod. Phys.* **57** 827
- [3] Abraham D B, Collet P, de Coninck J and Dunlop F 1990 *Phys. Rev. Lett.* **65** 195
- [4] Chopard B *J. Phys. A: Math. Gen.* to appear
- [5] Joanny J F and de Gennes P G 1986 *J. Physique* **47** 121
- [6] Abraham D B, Collet P, de Coninck J and Dunlop F *J. Stat. Phys.* in press
- [7] Edwards S F and Wilkinson D R 1982 *Proc. R. Soc. A* **381** 17
- [8] Wolf D E and Tang L-H 1990 *Phys. Rev. Lett.* **65** 1591
- [9] Family F 1986 *J. Phys. A: Math. Gen.* **19** L441
- [10] Aragao de Carvalho C and Caracciolo S 1983 *J. Physique* **44** 323
- [11] Stauffer D and Jan N 1988 *Can. J. Phys.* **66** 187